

N O T I C E

THIS DOCUMENT HAS BEEN REPRODUCED FROM
MICROFICHE. ALTHOUGH IT IS RECOGNIZED THAT
CERTAIN PORTIONS ARE ILLEGIBLE, IT IS BEING RELEASED
IN THE INTEREST OF MAKING AVAILABLE AS MUCH
INFORMATION AS POSSIBLE

EFFECT OF TANGENTIAL TRACTION AND ROUGHNESS ON CRACK
INITIATION/PROPAGATION DURING ROLLING CONTACT

by Norimune Soda* and Takashi Yamamoto**

National Aeronautics and Space Administration
Lewis Research Center
Cleveland, Ohio 44135

ABSTRACT

E-604

Rolling-fatigue tests of 0.45 percent carbon steel rollers were carried out using a four-roller type rolling contact fatigue tester. Tangential traction and surface roughness of the harder mating rollers were varied and their effect was studied. The results of the study indicate that the fatigue life decreases when traction is applied in the same direction as that of rolling. When the direction of traction is reversed, the life increases over that obtained with zero traction. The roughness of harder mating roller also has a marked influence on life. The smoother the mating roller, the longer the life. Microscopic observation of specimens revealed that the initiation of cracks during the early stages of life is more strongly influenced by the surface roughness, while the propagation of these cracks in the latter stages is affected mainly by the tangential traction.

INTRODUCTION

Rolling contact fatigue which occurs in rolling element bearings, gears and a number of other important mechanisms has long been a limiting parameter for the designer working with elements having concentrated contacts. The generally used criterion for defining the onset of the rolling contact fatigue is the normal contact stress.

*University of Tokyo, Tokyo, Japan.

**Tokyo University of Agriculture and Technology, Tokyo, Japan, and NRC-NASA Research Associate.

The rolling contact fatigue life, however, varies markedly with the presence of sliding and the roughness of the contact surfaces even when the applied normal load is kept constant.

In order to establish a more reliable criterion as well as to better comprehend the mechanism of rolling contact fatigue, an adequate explanation must be developed as to why the element experiencing sliding (this occurs on the slower of two elements in contact) should pit more readily and further why the life is influenced by the surface roughness.

It has been definitely demonstrated that the dependency of life on the slip/roll ratio is attributable to that of tangential traction. This is accomplished by analyses of the relationship of life, slip/roll ratio and tangential traction working at the contact surface when using a four-roller type rolling contact machine (1,2). In the present study the same machine was used. The effect of only a single factor, that is, roughness or tangential traction was extracted and studied independently.

With ordinary fatigue of metals the mechanism is frequently discussed from the metallurgical point of view. This view holds that fatigue consists of two processes, 1) fatigue crack initiation or formation and 2) propagation or crack growth (3). It has not yet been satisfactorily established whether both the mechanisms of ordinary fatigue and that of rolling contact fatigue are substantially the same or different. There have been an increasing number of publications in which attempts have been made to approach the rolling contact fatigue by differentiating between the two processes (4 to 9). In order to understand the mechanism of rolling contact fatigue, it is worthwhile to analyse all the experimental results of rolling contact fatigue from the aforementioned view point even if the approach is phenomenological and tentative.

In this paper, the effects of tangential traction and surface roughness on rolling contact fatigue life are determined and certain aspects of rolling contact fatigue cracks are analysed. The mechanism of rolling contact fatigue is discussed from the view point that the fatigue process consists of crack initiation and propagation.

APPARATUS

A four-roller type rolling contact machine was used in these studies. For most conventional test rigs, predetermined "apparent" slide/roll ratios are usually given between the rollers by controlling the rotational speeds with motors and dynamometers. The greater the surface roughness the more is the tangential traction even between the surfaces under the condition of constant slip/roll ratio. The tangential traction generally varies with the laph of time. This is due to the decrease in the diameter caused by plastic deformation or wear of the contacting surfaces. The slip/roll ratio is determined by the nominal rotational speeds of the components (10). The machine used in this study is free from such limitations.

A "center roller" is supported by the three "outer rollers" located every 120 degrees around the former, Fig. 1. The shaft of the two bottom outer rollers are supported by the bearings which are fixed to the frame. The top outer roller is mounted on the shaft which is supported by vertically movable bearings. A static load up to 450 kg can be applied to the shaft by weights. This allows the identical normal load to be placed on the three contacts.

The rotational speeds of both the center and the outer rollers were positively controlled by separate driving systems to attain a pure rolling condition or any desired slip/roll ratio. The center roller is connected directly to a torque transducer, and then to a d.c. electric motor/dyna-

momenter. The three outer rollers are driven through a gearing at identical speeds by another motor/dynamometer. The torque transducer allows an accurate measurement of the tangential traction working on the contact points.

An acceleration detector is attached to the loading mechanism for determining the rolling contact fatigue life. For lubrication, a drip feed system is used which feeds lubricating oil onto the top outer roller at a rate of about 10 cc per minute.

SPECIMENS

Life of and fatigue cracks in the center roller are determined. Rollers made of 0.45 percent C plain carbon steel are used as the "center roller." The rollers were machined from rods which were hardened and annealed to 200 diamond pyramid hardness, the dimension of which is 40 mm in diameter and 10 mm in width, Fig. 2. Surfaces were finish ground circumferentially, being 1 μm in their peak-to-valley roughness. The composition and properties of the material are listed in Table 1.

In most experiments mating outer rollers are made of JIS SUJ2 (equivalent to AISI 52100 steel), the dimension of which are 40 mm in diameter and 9 mm in width. The rollers were hardened to 700-800 diamond pyramid hardness. Surfaces were finished circumferentially by emery papers to 0.1, 0.5 and 1.0 μm in peak-to-valley roughness.

In some experiments, combinations of the center roller, 9 mm in width and the outer rollers, 10 mm in width were adapted. However, the contact width is the same, 9 mm for all experiments.

PROCEDURE

The test rollers were mounted on the apparatus after being cleaned by washing with naphtha and trichloroethylene. The speed of the center roller was kept constant at 1500 rpm throughout the experiment, while those of the

outer rollers were controlled to give any desired tangential traction. The normal load applied was 303 kg. The maximum Hertzian pressure at this load is 112 kg/mm^2 . Straight mineral oil was used as lubricant. Lubricant viscosity is listed in Table 2.

Life of rolling contact fatigue elements is determined as follows. Once pitting has appeared on the roller surface, the process accelerates. The acceleration detecting system brings the apparatus to a halt and the fatigue life is then determined. An acceleration level of 2G has been arbitrarily chosen at which the detecting mechanism operates. This does not cause a serious error because the pitting accelerates to a high value quickly. All tests were carried out in the laboratory atmosphere. The approximate temperature was 20°C , and the approximate relative humidity was 70 percent. Tangential traction is determined as T/R , where R is the radius of rollers and T is the torque transmitted at the contact point.

All the cracks observed in this study were of a surface origin. The size of a propagated crack was determined by the length measured in the axial direction of the crack opened to the contact surface and the distance of the crack tip from the surface.

For the observation of fatigue cracks at the contact surface, the center roller was taken out after every $3-5 \times 10^4$ cycles of contact and washed, then photomicrographed. The roller was again mounted on the apparatus and the same procedure was repeated throughout its life. Photomicrographs of the plane sectioned perpendicular to the axis of the roller were taken for the observation of the propagated cracks.

The distance of a crack tip from the surface was estimated by measuring the maximum thickness of the surface layer beyond which the tip of the

largest crack does not reach. The surface layer was removed continuously by lapping until the largest crack disappeared.

In this paper, the sliding was represented by the torque or tangential traction transmitted between the center roller and the outer roller. "Positive" implies that the tangential traction is coincident with the direction of rolling, which is also defined as "follower." "Negative" implies the inverse, which is defined as "driver." Hitherto the terminology of so-called "negative sliding" has been used frequently. This is defined as that which occurs on the slower of two elements in contact. In Fig. 3 the comparison of the terminologies is indicated between conventional terminology and that used herein.

RESULTS

It is well known that the rolling contact fatigue life decreases markedly with an increase of so-called "negative sliding." What then, is the life under the condition of "positive sliding," which is defined in terms of the faster of the two elements in contact? The results are shown in Table 3. In these experiments, both center and outer rollers are made of 0.45 percent C plain carbon steel. The driver survives the followers of from 30-80 times longer and does not fracture on the surface at all.

The relationship between life and the tangential traction which was chosen over a particular range of both "negative sliding" and "positive sliding" is shown in Fig. 4, together with a parameter for the roughness of harder mating outer rollers. The life varies markedly according to the direction and the magnitude of the torque, or tangential traction. The life increases uniformly with the tangential traction approaching the "positive sliding" region, which is the situation where one has negative tangential

traction. Figure 4 also shows definitely that the surface roughness of harder mating roller influences remarkably rolling contact fatigue life.

In Fig. 5 the relationship between the life and the roughness is plotted on the log-log axes. It should be noted that a 10 times reduction in the surface roughness gives an increased life in terms of cycles to pitting of 10 times.

The representative aspects of micro-cracks formed at the contact surfaces are shown in Fig. 6. The roughness of harder mating roller is 1.0, 0.5 and 0.1 μm in peak-to-valley roughness, respectively. The figures at the right side are high magnification photographs of the area marked by the solid line on the surfaces after 9.0×10^3 cycles of contact. Micro-cracks appear in the early stages with an increase of roughness of the harder mating roller, which corresponds closely to the behavior of the roughness dependent rolling contact fatigue life shown in Figs. 4 and 5. However, there is no difference in the phenomenon of crack formation among the drivers, the pure rolling rollers and the followers. Symbol D. R. represents the direction of rolling and D. T. the direction of tangential traction working at the contact surface. Figure 7 shows an example of a series of a propagating crack taken at frequent intervals during life to pitting failure. From the results a fan-shaped crack is clearly visible at the surface in less than one-half of the life to pitting. In this particular case the estimated life is 6.5×10^5 cycles of contact. Similar observations were made for other conditions of tangential traction.

The relationship between the axial length and circumferential width of the propagated crack that opened on the contact surface and the cycles of contact are presented in Fig. 8. With the followers, the crack propagation rate, which is defined as a ratio of the increment of the axial length of

the crack to the cycles of contact necessary for the crack growth, is larger than that of the drivers. At the contact surface, usually several cracks were found having different crack propagation rates. Under certain conditions of negative tangential traction, i.e., in the case of the driver, there was a situation observed in which the size of the crack shrinks, getting smaller and smaller. Figure 8 are examples presented for reference purposes. In this study attention was paid to the greatest rate of crack propagation in the roller. Figure 8 also shows positive evidence that a positive tangential traction tends to increase the crack propagation rate over that of the case of no tangential traction. The opposite is also true if the direction of traction is reversed.

Turning now to the question how deep does the crack tip reach beneath the surface, Fig. 9 shows the initial micro-cracks both at the surface and in the subsurface layer for the specimen shown in Fig. 6. These micro-cracks disappear after a layer of 4 μm in depth is removed from the surface.

A typical propagated fan-shaped micro-crack is shown in Fig. 10. The left-hand micrograph indicates the entire crack before sectioning. The right-hand photo shows the shape of the crack after sectioning the roller near the center of the crack perpendicular to the axis. The fan-shaped micro-crack is visible; the tip does not reach the layers where the maximum shear stress or the maximum alternating shear stress occurs. The maximum shear stress occurs at a depth of 150 μm , and the maximum alternating shear stress at a depth of 70 μm .

Figure 11 presents examples of small cracks that appeared on the surface of the follower and the driver in the early stages of failure. Both cracks are similar in shape except near the tip. The size of the crack for

the driver is larger than that for the follower. This is so because the crack of the driver is found at a more progressed stage. Figure 11 also presents no distinct relation between the profile of crack and the plastic flow pattern of the material in the axial plane.

All cracks observed in this study are recognized as surface originated ones which propagate into the substrate. A representative relation between the distance of the crack tip from the surface and the cycles of contact is shown in Fig. 12. The roughness of harder mating roller is $0.5 \mu\text{m}$ in peak-to-valley roughness and the tangential torque is 5 kg-cm and -5 kg-cm , respectively. There are observed two phenomena, i.e., a low propagation rate phenomenon and a high propagation rate one. For the case of the low propagation rate, the rate is independent of the tangential traction, which appears to be related to the micro-cracks which form during the crack initiation process of rolling contact fatigue. In the case of high propagation rate, however, it is dependent on the tangential traction which corresponds well with the results of Fig. 8.

From the aforementioned results, it may be concluded that both the effect of roughness and the tangential traction on rolling contact fatigue can be understood if fatigue is considered to consist of two processes, that is, crack initiation and propagation. The former is related to the roughness, and the latter is distinctly related to the tangential traction.

DISCUSSION

The mechanism of rolling contact fatigue has been explained in terms of several sources of stress concentration within the macroscopic contact stress field. In the subsurface region, hard nonmetallic oxide inclusions, structural changes, etc. have been regarded as predominant stress raisers, and sites at which fatigue cracks originate (11 to 13). On the other hand,

it has been pointed out that with high purity steels there is a shift with the predominant fatigue damage originating at the surface. With rolling contact components made of softer material, such as gears and cams, the fatigue is therefore essentially surface-initiated. Taking into consideration a wide variety of the aspects of rolling contact fatigue, the mechanism has been discussed with the aid of several competitive modes of damage.

The microscopic examination of failed 0.45 percent carbon steel rollers has not revealed any relationship between fatigue cracks and subsurface inclusions. Micro-cracks always appear first at the surface and propagate into the substrate of the roller. The mechanism of surface originated types of rolling contact fatigue can be explained in terms of surface flaws that may serve as the prime source for local stress intensification leading to surface cracking. In this study surface asperities of the harder mating roller act as stress raisers for testing rollers.

Figure 13 presents some examples of strain hardening occurring on the surface and in the subsurface after a certain number of cycles of contact. Two distinct hardening regions can be observed. The first has its maximum at the surface and shows a sharp decrease in hardness with the distance from the surface. The second is broader and similar to that of the static maximum shear stress given by the Hertz theory for smooth surfaces. Effects of the roughness of harder mating roller is more evident in the first region than in the second, Fig. 13(b). On the other hand, the effect of the tangential traction is not noticeable in the distribution of strain hardening, Fig. 13(c). Stress concentration caused by asperities at the surface is recognized quantitatively in the surface layer in photoelastic fringe pattern of Fig. 14.

Strain hardening can be taken as a measure of the deterioration, since more damage must have been accumulated in a strain hardened material. It, therefore, has a higher possibility of initiating microscopic cracks as shown in Fig. 6. Regimes of severe strain hardening appear adjacent to and at some distance from the surface in the material after rolling contact. This may be explained by a simplified stress analysis. Except for the case of perfect EHD lubrication, most load is supported by a number of real contact points, and Hertzian contact pressure is nothing but the local average of the loads working on these minute contact points. Thus, the load shared by a number of real contacts develops localized stress fields in a thin layer adjacent to the surface, and the averaged Hertzian pressure develops a broader stress field in the material beneath it. The stress patterns in these two regimes result in a pattern of strain hardening as described earlier.

The comparison between strain hardening and subsurface plastic flow for the results of Table 3 is shown in Fig. 15. Hardness of the driver is larger owing to receiving larger number of repetitive contacts than the follower.

As mentioned in the description of the results (Table 3) pitting or flaking does not occur at all at the surface of the driver. The phenomenon may be explained from the pattern of the subsurface plastic flow and the effects of the tangential traction. Micro-cracks initiated at the surface by repetitive contact can propagate into the substrate, if some requirement is not satisfied concerning the tangential traction. With rolling contact fatigue, the crack has a tendency to propagate into the thin surface layer in the direction of rolling at an angle of about 20-30 degrees to the surface, putting its tip toward the direction of movement of normal load,

i.e., the inverse direction of rolling. This phenomenon has not yet been explained satisfactorily. The direction of crack propagation is not merely influenced by the direction of tangential traction in the thin surface layer. As shown in the etched photographs, Fig. 15, the direction of plastic flow does not appear to correspond to the direction of the locus of crack propagation. This disagreement in direction may act as one of retardations for crack propagation into the substrate for the case of the driver. One possible reason for the higher fatigue life for the driver may be related to this observation.

CONCLUSION

An experiment is described on rolling contact fatigue for 0.45 percent carbon steel rollers during lubricated rolling contact with varying tangential traction and surface roughness of the mating rollers.

The fatigue life decreases when a tangential traction is applied in the same direction as that of rolling. When the direction of traction is reversed, the life increases over that obtained under zero traction. The roughness of harder mating roller has a marked influence on the life. The smoother the mating roller, the longer the life. Micrographs of the surface of the rollers and sectioned specimens reveal that microscopic cracks leading to rolling contact fatigue initiate at the surface or in a thin subsurface layer. The initiation of cracks during the early stages of life is more strongly influenced by the surface roughness, and the propagation of these cracks in the latter stages is affected mainly by the tangential traction. The direction of the locus of crack propagation does not appear to correspond to the direction of subsurface plastic flow. This disagreement in direction may act as one of retarding forces for crack propagation into the substrate of the driver.

REFERENCES

1. Soda, N., Yamashita, M. and Osora, K., "Effect of Tangential Force on Rolling Fatigue," J. Jpn. Soc. Lubr. Eng., 16, 8, pp 573-580 (1971).
2. Soda, N. and Yamamoto, T., "Effects of Tangential Traction and Surface Roughness of Mating Roller of Cr-Mo Steel on Rolling-Fatigue Life at 0.45 percent Carbon Steel," JSLE-ASLE International Lubrication Conference, ed. by T. Sakurai, pp 458-465 (1975).
3. Honeycombe, R. W. K., The Plastic Deformation of Metals, St. Martin's Press, Inc., New York (1968), p 411 and 420.
4. Way, S., "Pitting Due to Rolling Contact," J. Appl. Mech., 2, 2, pp A-49 - A-58 (1935).
5. Martin, J. A. and Eberhardt, A. D., "Identification of Potential Failure Nuclei in Rolling Contact Fatigue," ASME Trans., 89, pp 932-942 (1967).
6. Borgese, S., "An Electron Fractographic Study of Spalls Formed in Rolling Contact," ASME Trans., 89, pp 943-948 (1967).
7. Dawson, P. H., "Rolling Contact Fatigue Crack Initiation in a 0.3 Percent Carbon Steel," Proc. Inst. Mech. Eng., London, 183, Pt. 1, 4, pp 75-86 (1968-69).
8. Littmann, W. E., Widner, R. L., Wolfe, J. O., and Stover, J. D., "The Role of Lubrication in Propagation of Contact Fatigue Cracks," ASME Trans., 90, pp 89-100 (1968).
9. Syniuta, W. D. and Corrow, C. J., "A Scanning Electron Microscope Fractographic Study of Rolling-Contact Fatigue," Wear, 15, pp 187-199 (1970).
10. Soda, N. and Yamamoto, T., "A Consideration on Rolling-Sliding Friction with Very Small Slip Ratio and Its Related Problems," J. Jpn. Soc. Lubr. Eng., 21, 7, pp 441-446 (1976).

11. Kuroda, M., "The Relation Between the Quality of Bearing Steel and Rolling Fatigue Life," J. Jpn. Soc. Mech. Eng., 63, pp 1442-1451 (1960).
12. O'Brien, J. L. and King, A. H., "Electron Microscopy of Stress-Induced Structural Alteration Near Inclusions in Bearing Steels," ASME Trans., 88, pp 568-572 (1966).
13. Martin, J. A., Borgese, S. F., and Eberhardt, A. D., "Microstructural Alterations of Rolling Bearing Steel Undergoing Cyclic Stressing," ASME Trans., 88, pp 555-567 (1966).

TABLE 1. - COMPOSITION AND PROPERTIES OF 0.45 PERCENT C
PLAIN CARBON STEEL

Analysis, percent								Strength	
C	Si	Mn	P	S	Cu	Ni	Cr	Yield, kg/mm ²	Tensile, kg/mm ²
0.45	0.25	0.76	0.013	0.023	0.03	0.016	0.040	59	77

TABLE 2. - VISCOSITY OF LUBRICANT

Temperature, °F	Viscosity, cSt
100	9.8
200	2.3

TABLE 3. - COMPARISON OF LIFE OF THE
FOLLOWER WITH THE DRIVER

Follower life			Driver life
2.1x10 ⁶	3.1	1.7	^a 4.8x10 ⁷ (not fatigued)
2.3	.8	1.2	
2.3	1.4	1.3	
2.0	1.9	.9	
2.1	.3	1.3	
3.1	1.8	.8	
1.6	2.1	.8	
1.5	1.6	.8	
2.3	2.5	.6	

^aSlip/roll ratio, 0.7 percent; torque,
16 kg-cm ($\mu = 0.0026$).

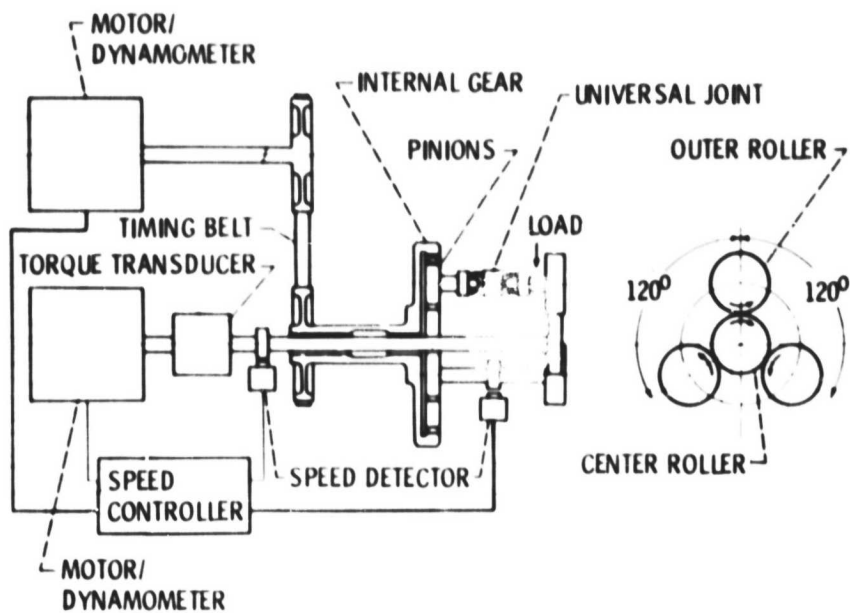
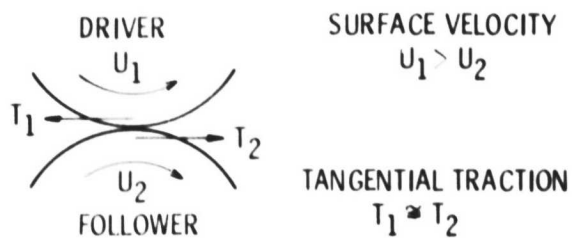


Figure 1. - Schematic diagram of the four-roller machine.



40 mm

Figure 2. - Specimens.



TERMINOLOGY

	CONVENTIONAL	PRESENT
FOLLOWER	NEGATIVE SLIDING	POSITIVE TANGENTIAL TRACTION
DRIVER	POSITIVE SLIDING	NEGATIVE TANGENTIAL TRACTION

Figure 3. - Definition of direction of tangential traction.

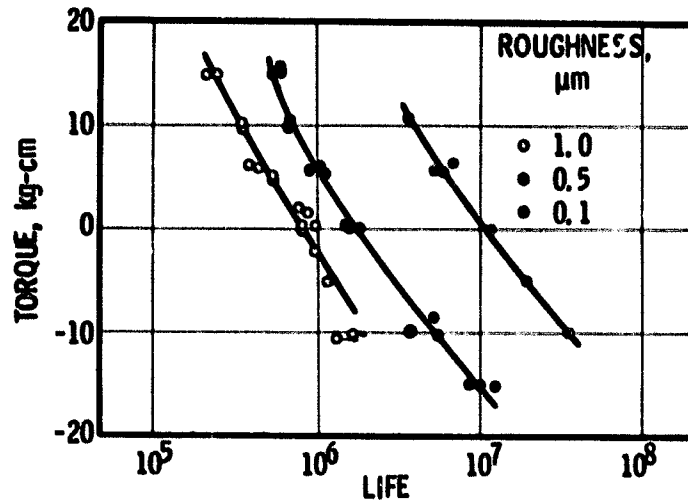


Figure 4. - Rolling fatigue life of a 0.45% C steel roller vs. tangential traction (represented with torque) for various roughness of mating JIS SUJ2 (equivalent to AISI 52100) roller. Roughness is represented with peak to valley distance.

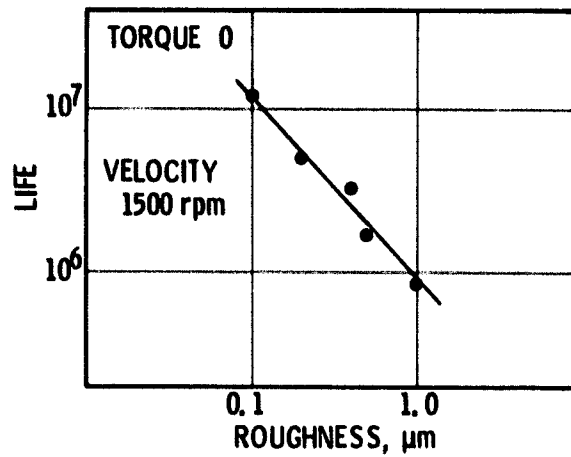
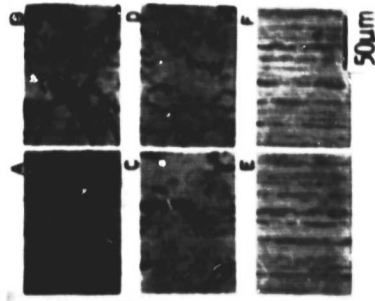


Figure 5. - Rolling fatigue life vs. roughness of harder mating roller.

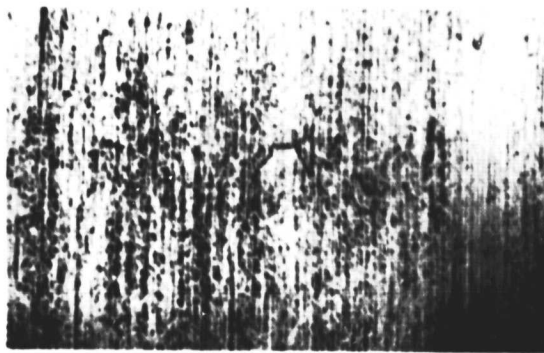
CYCLES OR CONTACT	ROUGHNESS 1.0µm		0.5µm		1.0µm	
	follower	driver	follower	driver	follower	driver
0						
90x10 ⁶						
30x10 ⁶						
10x10 ⁶						
45x10 ⁶						
TORQUE ±5 kg-cm						
		D.T.		D.R.		
		↑		↑		
		D.T.		D.R.		
		↑		↑		



D. R.: DIRECTION OF ROLLING
D. T.: DIRECTION OF TANGENTIAL TRACTION

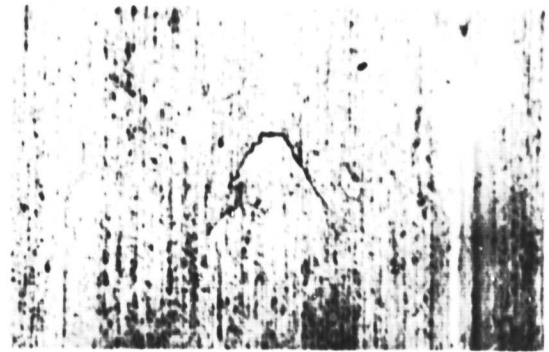
Figure 6. --Aspects of the initiation of micro-cracks at the surface.

ORIGINAL PAGE IS
OF POOR QUALITY

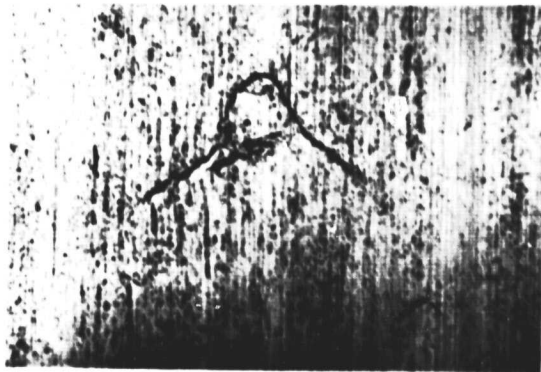


3.0×10^5 CYCLES

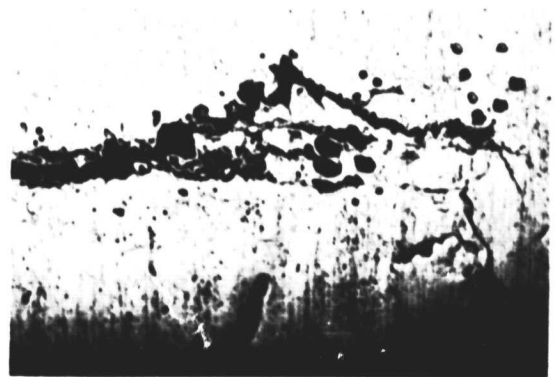
D.R. ↑
D.T. ↑



3.6×10^5 CYCLES



3.9×10^5 CYCLES



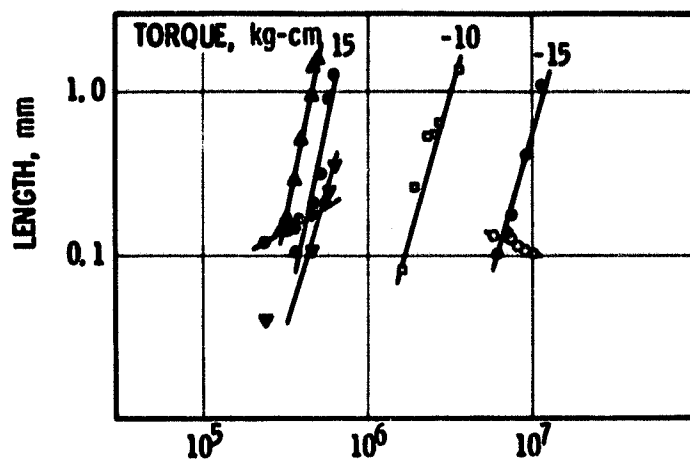
5.8×10^5 CYCLES

0.5 mm

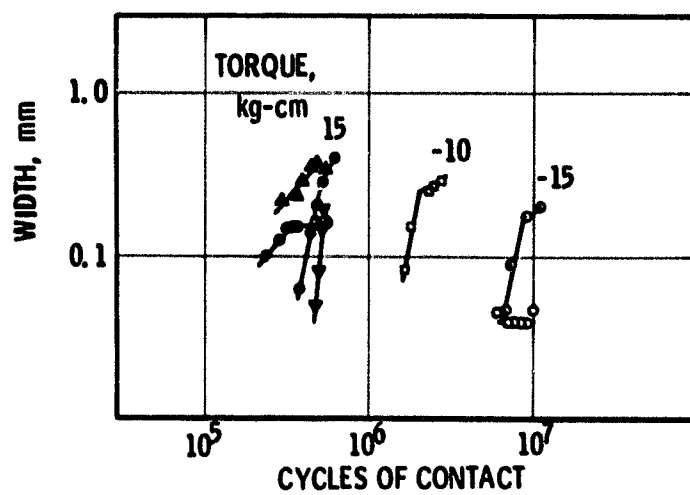
TORQUE; 15 kg-cm (FOLLOWER)
ROUGHNESS; $0.5 \mu\text{m}$

Figure 7. - An example of crack propagation.

ORIGINAL PAGE IS
OF POOR QUALITY

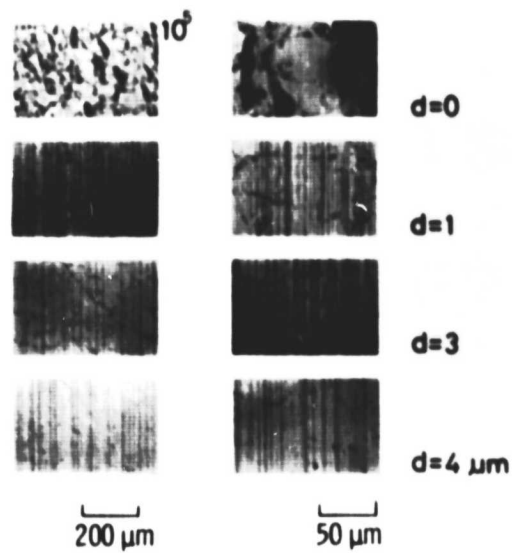


(a) AXIAL LENGTH.



(b) CIRCUMFERENTIAL WIDTH.

Figure 8. - Size of fatigue crack at the surface vs. cycles of contact for various tangential traction.



d; THICKNESS OF SURFACE LAYER
REMOVED BY LAPPING

Figure 9. - Micro-cracks at the initial surface
and in the subsurface layer.

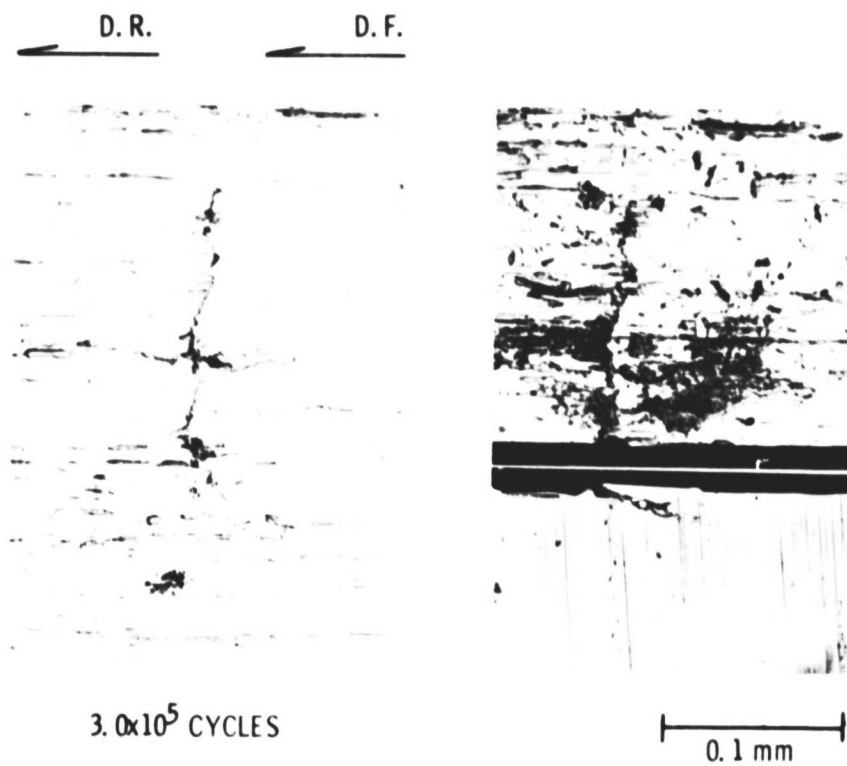
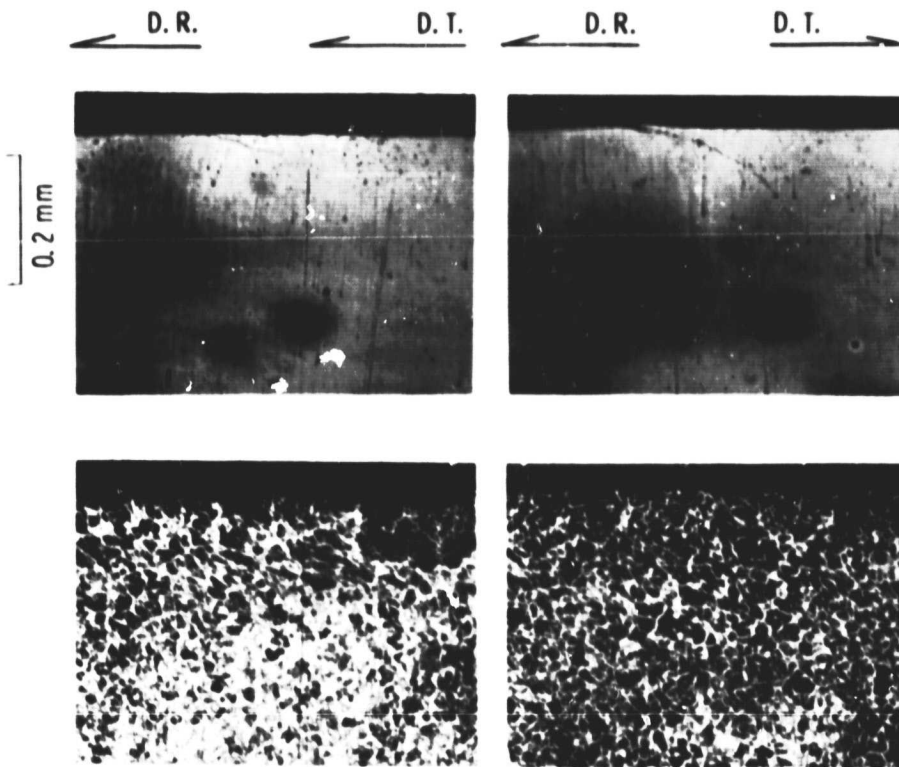


Figure 10. - Aspect of propagated micro-crack.



(a) FOLLOWER; 4.4×10^5 CYCLES
TORQUE; 15 kg-cm

(b) DRIVER; 2.88×10^6 CYCLES
TORQUE; -10 kg-cm

Figure 11. - Examples of visible small cracks for the follower and the driver sectioned at the center of the crack.

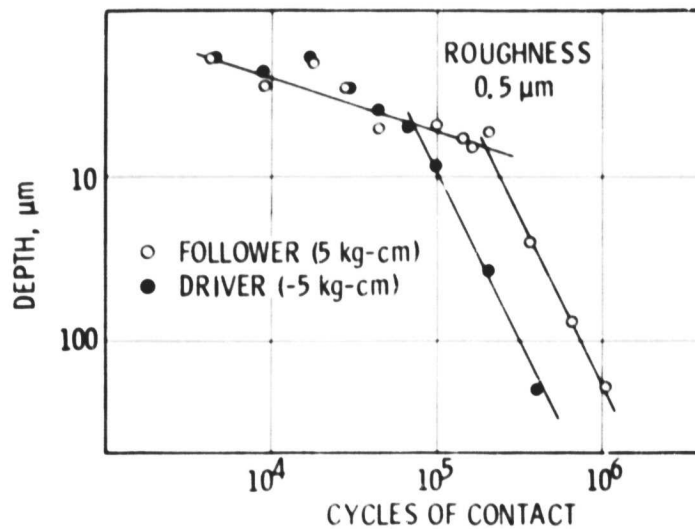


Figure 12. - Distance of crack tip from the surface vs. cycles of contact.

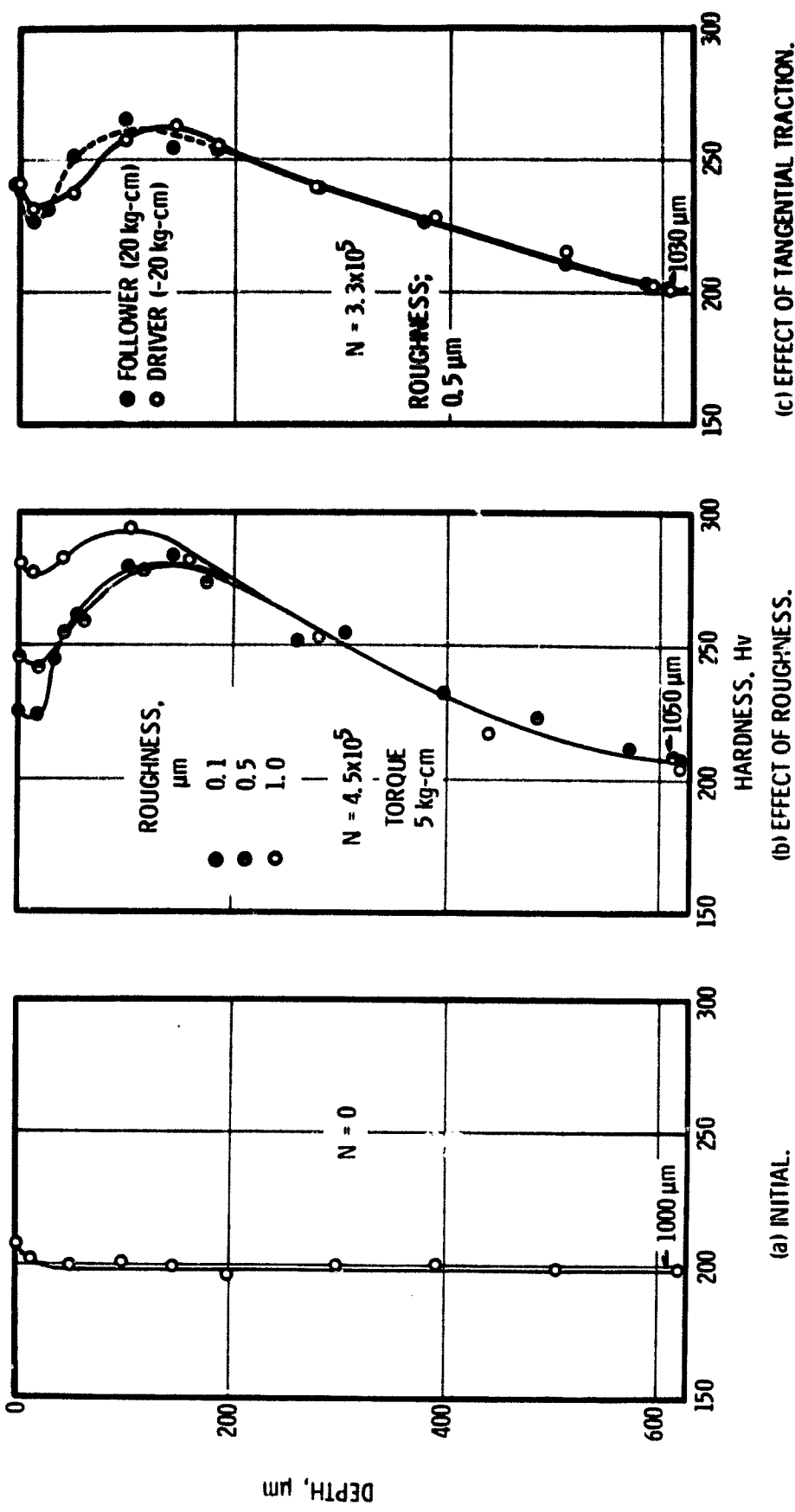
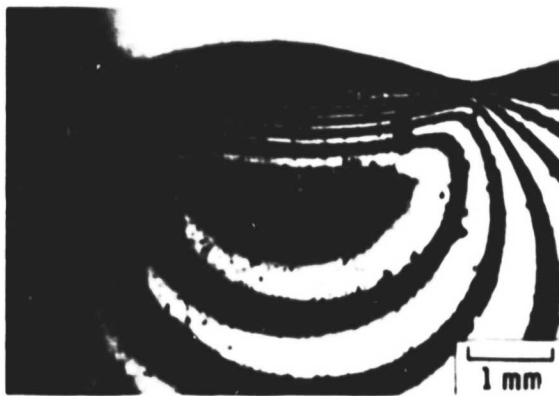


Figure 13. - Variation of microhardness with subsurface depth.

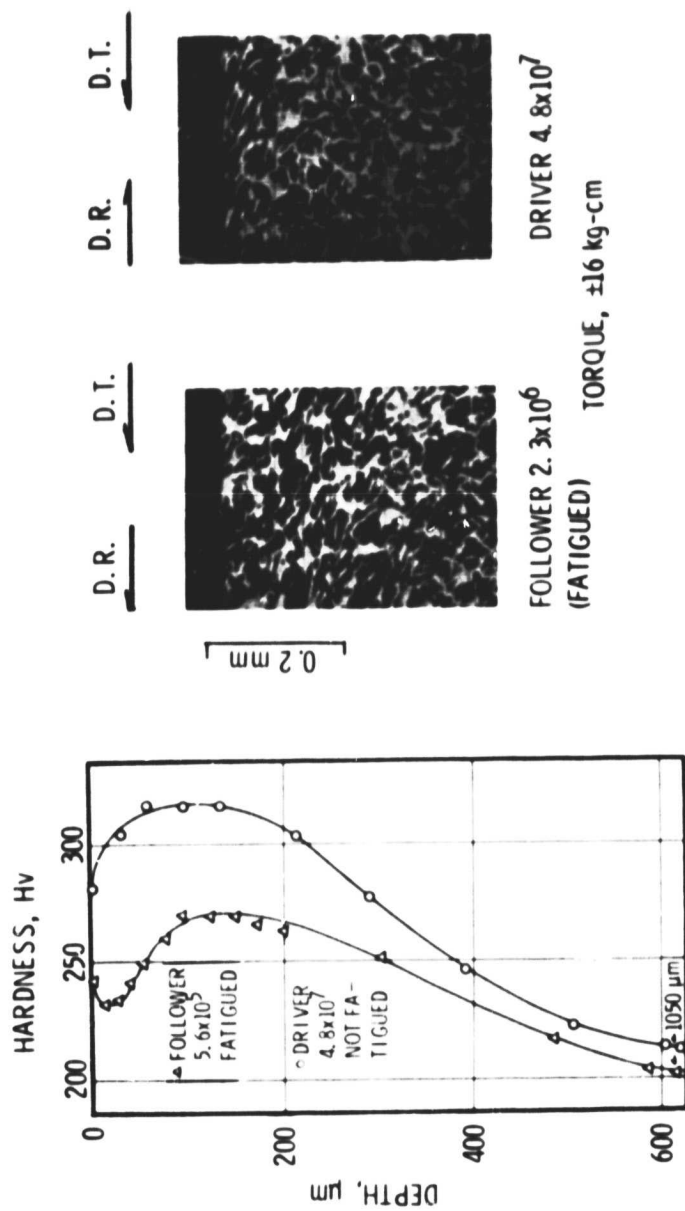


(a) ROUGHNESS OF EPOXY RESIN; 8 μm .

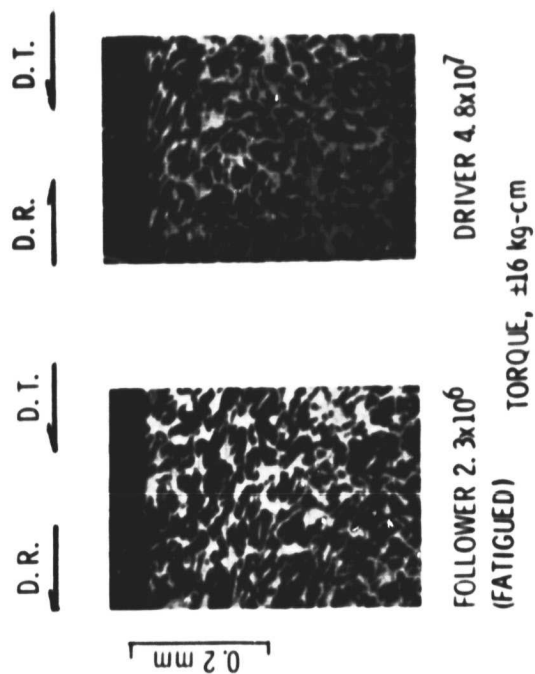


(b) ROUGHNESS OF EPOXY RESIN; 0.5 μm .
ROUGHNESS OF MATING ROLLER; 0.5 μm
"CLASSIC" MAXIMUM HERTZIAN PRESSURE;
1.9 kg/mm^2

Figure 14. - Effect of roughness on photo-elastic fringe pattern (isochromatics).



(a) STRAIN HARDENING.



(b) SUBSURFACE PLASTIC FLOW.

Figure 15. - Strain hardening and subsurface plastic flow for the results of table III.